Heterocycles

DOI: 10.1002/ange.201400068

# On-Top π-Stacking of Quasiplanar Molecules in Hole-Transporting Materials: Inducing Anisotropic Carrier Mobility in Amorphous Films**

*Atsushi Wakamiya,* Hidetaka Nishimura, Tatsuya Fukushima, Furitsu Suzuki, Akinori Saeki, Shu Seki, Itaru Osaka, Takahiro Sasamori, Michihisa Murata, Yasujiro Murata,* and Hironori Kaji**

***Abstract:*** *Dimers of partially oxygen-bridged triarylamines were designed and synthesized as hole-transporting materials. X-ray structural analyses revealed that these compounds form on-top π-stacking aggregates in the crystalline state. TRMC measurements showed that high levels of anisotropic charge transport were induced in the direction of the π-stacking. Surprisingly, even in vacuum-deposited amorphous films, these compounds retained some of the face-on π-stacking, thus facilitating an out-of-plane carrier mobility.*

The development and characterization of improved charge-transporting materials still remains a crucial issue for the achievement of high-performance organic devices, for example, for organic light-emitting diodes (OLEDs),[1] organic field-effect transistors (OFETs),[2] and organic photovoltaics (OPVs).[3] Efficient charge transport in molecular solids requires charges to move easily from molecule to molecule.[4] In the molecular design of these materials, it is therefore important not only to control the π-electronic structure for tuning the HOMO and LUMO levels and lowering of the reorganization energy ($\lambda$), but also to control the packing structure in the solid state to facilitate large charge transfer integrals ($J$). Acenes, such as pentacene, are widely used as charge-transporting materials in OFETs, because of their rigid π-conjugated skeletons with high planarity. In the solid state, pentacene adopts a herringbone structure with a tilted molecular arrangement, which is the result of π-π interactions and the presence of CH-π interactions (electrostatic interaction).[5] Introducing substituents in the peri-position of acenes or increasing the C/H ratio in the ring-fused aromatic compounds can be effective strategies for a molecular design in which CH-π interactions are prevented and a better packing motif with facilitated charge mobility is obtained.[2,6] However, molecular design approaches that allow effective control over the molecular orientation in the solid state remain limited. Representative examples for hole-transporting materials used in OLEDs are triarylamines with propeller-like structures, such as TPD[7a] and α-NPD.[7b] These materials are used as amorphous films, and the conformations of individual molecules as well as of their aggregates have not been determined unambiguously, thus rendering precise conclusions regarding molecular design strategies difficult.[8] Accordingly, the elucidation of the exact relationship between the molecular orientation in the crystalline and amorphous state remains a key challenge to be addressed in the design of advanced charge-transporting materials.

In this study, we focused on partially bridged triarylamines as the π-conjugated skeletons for the charge-transporting materials. In these amines, three phenyl groups are constrained in a quasiplanar fashion by two oxygen bridges (Figure 1). We envisioned that the use of quasiplanar scaffolds should be beneficial to provide: a) delocalized π-conjugation by enhanced planarity, and b) dense π-stacking in the solid state, arising from slightly twisted molecular structures. In addition, the dispersion in the direction of the C–H bonds in the lateral position of the quasiplanar molecules should decrease the contribution of the CH-π interactions between neighboring molecules, so that on-top π-

[*] Prof. Dr. A. Wakamiya, H. Nishimura, Dr. T. Fukushima, F. Suzuki, Prof. Dr. T. Sasamori, Dr. M. Murata, Prof. Dr. Y. Murata, Prof. Dr. H. Kaji
Institute for Chemical Research, Kyoto University
Uji, Kyoto 611-0011 (Japan)
E-mail: wakamiya@scl.kyoto-u.ac.jp
yasujiro@scl.kyoto-u.ac.jp
kaji@scl.kyoto-u.ac.jp
Dr. A. Saeki, Prof. Dr. S. Seki
Department of Applied Chemistry
Graduate School of Engineering, Osaka University
2-1 Yamadaoka, Suita, Osaka 565-0871 (Japan)
Dr. I. Osaka
Emergent Molecular Function Research Group, RIKEN CEMS
Wako, Saitama 351-0198 (Japan)
Prof. Dr. A. Wakamiya
Precursory Research for Embryonic Science and Technology (PRESTO) (Japan) Science and Technology Agency
4-1-8 Honcho, Kawaguchi, Saitama 332-0012 (Japan)

[**] This work was partially supported by JST and the Collaborative Research Program at the ICR, Kyoto Univ. Support was also received from the Funding Program for World Leading Innovative R&D on Science and Technology (FIRST Program). The NMR measurements were supported by the Joint Usage/Research Center (JURC) at the ICR, Kyoto Univ. Synchrotron single-crystal X-ray analysis was carried out with the SPring-8 beam line BL38B1 with the approval of JASRI (2012A1448, 2012B1319, and 2013A1489). 2D GIXD experiments were performed at BL19B2 of SPring-8 with the approval of JASRI (2013A1634). We thank Dr. T. Koganezawa (JASRI) for advice on the 2D GIXD measurements.

Supporting information for this article is available on the WWW under http://dx.doi.org/10.1002/anie.201400068.

  

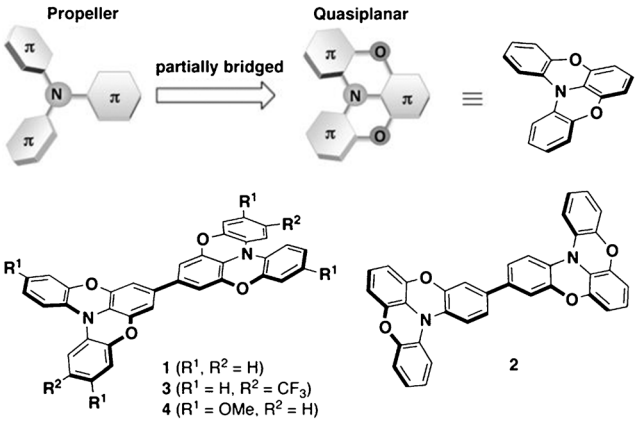


***Figure 1.*** Molecular design aspects for charge-transporting materials with a quasiplanar structure as the key feature.

stacking could be facilitated in the solid state. As model compounds, we designed and synthesized a series of partially oxygen-bridged triarylamine dimers **1**–**4** (Figure 1). Herein, we report on the characterization of **1**–**4** in solution and the solid state, as well as on the relationship between the packing structures and the anisotropic charge-carrier-transport properties, which were observed for **1** and **2** both in the crystalline and amorphous states.

The key reaction step to establish quasiplanar structures in **8a–c** is a twofold intramolecular nucleophilic aromatic substitution (Scheme 1a). Compounds **7a–c** were prepared by Ullmann reactions of **5a** or **5b** and **6a** or **6b** (61–68%). After removal of the protecting methyl groups in **7a–c** with $BBr_3$, a subsequent treatment with $K_2CO_3$ in DMF at 100°C resulted in the formation of cyclized products **8a–c** (67–95%). This synthetic route is straightforward, based on commercially available starting materials, and can be easily scaled up. In contrast to a previously reported synthetic route for **8a** via the linear intermediate 2,6-bis(2-bromophenoxy)aniline,[9] our route allows the preparation of derivatives containing substituents in the desired positions. For example, the bromination of triarylamine **7a** with 1 equiv of NBS resulted in the selective formation of **9** (75%). The subsequent twofold cyclization of **9** gave monobrominated **10**, an isomer of **8b**, in almost quantitative yield. The unsymmetric triarylamine **13** was obtained from two successive coupling reactions of **6b** with different aryl components. $Pd^0$-catalyzed arylation of **5a** with **6b** resulted in the selective formation of **11** (68%). A subsequent second Ullmann arylation afforded **12** (75%), which was doubly cyclized to give **13** (65%). Homocoupling of brominated **8b**, **8c**, **10**, and **13** yielded the corresponding dimers **1**–**4** (54–98%) as pale yellow solids (Scheme 1b).

The electrochemical and photophysical data as well as thermal analyses for **1**–**4** are summarized in Table 1. A detailed discussion of these properties can be found in the Supporting Information.

The optimized structures of **1**–**4**, calculated at the B3LYP/6-31G(d) level of theory, supported the expected quasiplanar structures for the partially oxygen-bridged triarylamine moieties (see Figure S17 in the Supporting Information). The HOMOs of **1**–**4** are highly delocalized over the whole π-skeleton (see Figure S18 in the Supporting Information), which allows effective tuning of the HOMO levels through the peripheral substituents on the outer phenyl rings. Fully delocalized HOMOs should also lower the reorganization energies of the hole transfer. For **1**–**4**, these were calculated at the B3LYP/6-31G(d) level to be lower (**1**: $\lambda^+ = 0.15$ eV; **2**: 0.15 eV; **3**: 0.18 eV; **4**: 0.17 eV) than those for TPD ($\lambda^+ = 0.26$ eV) or α-NPD ($\lambda^+ = 0.28$ eV).

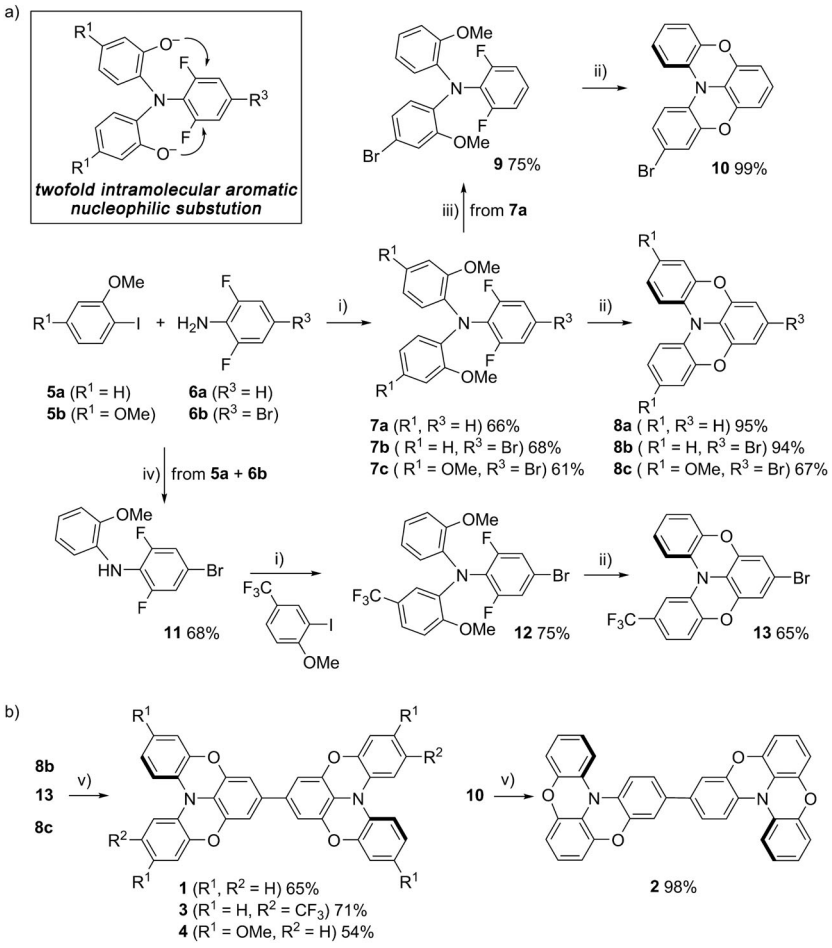


***Scheme 1.*** Reagents/conditions: i) Cu, $K_2CO_3$, *o*-dichlorobenzene, 180°C; ii) 1. $BBr_3$, $CH_2Cl_2$, 2. $K_2CO_3$, DMF, 100°C, (then $CH_3I$, 60°C for **8c**); iii) NBS (1 equiv), $CHCl_3$/AcOH, iv) $[Pd_2(dba)_3]\cdot CHCl_3$, P(*t*Bu)$_3$, NaO*t*Bu, toluene, 100°C; v) $[Ni(cod)_2]$, bipyridine, cod, THF, 60°C. NBS = *N*-bromosuccinimide, dba = *trans*,*trans*-dibenzylideneacetone, cod = cycloocta-1,5-diene.

***Table 1:*** Thermal analysis, electrochemical, and photophysical data for **1**–**4**.

| | $T_{d5}$[a] [°C] | $T_g$[b] [°C] | $E_{1/2,\,ox}$[c] [V] | IP[d] [eV] | $A$[e] [nm] (log ε) | $FL_{liq}$[e] [nm] ($\Phi$)[g] | $FL_{sol}$[f] [nm] ($\Phi$)[g] |
|---|---|---|---|---|---|---|---|
| **1** | 449 | 64 | +0.25 +0.44 | 5.05 | 387 (4.22) | 451 (0.51) | 491 (0.40) |
| **2** | 441 | 123 | +0.23 +0.42 | 5.03 | 397 (4.48) | 449 (0.69) | 508 (0.51) |
| **3** | 408 | 56 | +0.41 +0.58 | 5.21 | 385 (4.16) | 439 (0.45) | 485 (0.14) |
| **4** | 443 | 34 | +0.02 +0.17 +0.86[h] | 4.82 | 405 (4.10) | 489 (0.77) | 533 (0.19) |

[a] 5% weight loss temperature measured by thermogravimetric analysis (TGA). [b] Glass transition temperature measured by differential scanning calorimetry (DSC). [c] Half-wave oxidation potential (versus $Fc/Fc^+$) measured by cyclic voltammetry in $CH_2Cl_2$ (0.3 mM) with $[(n\text{Bu})_4\text{N}][PF_6]$ (0.1 M) as the supporting electrolyte. [d] Estimated ionization potentials (IPs) from the first oxidation potential (+4.80 eV).[10] [e] UV absorption/fluorescence measured in $CH_2Cl_2$. [f] Fluorescence measured in the solid state (ground crystals). [g] Absolute quantum yields determined by a calibrated sphere system. [h] Corresponding to a two-electron oxidation.

Single crystals of **1**–**4** suitable for X-ray diffraction analysis were obtained by sublimation or recrystallization. The structural analysis confirmed quasiplanar structures for dimers **1**–**4** in the crystalline state. For example, the dihedral angles between the outer and inner phenyl rings in **1** (18.6°/23.0°; see Figure 2a) are in good agreement with the

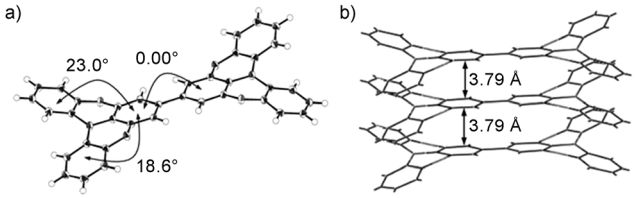


***Figure 2.*** X-ray crystal structure of **1**: a) ORTEP drawing (50% probability for thermal ellipsoids) and b) packing structure.

calculated optimized structure (22.8°). However, the dihedral angles between the inner phenyl rings obtained from the optimized structures of **1**–**4** (33.8–35.1°) are not consistent with those observed in the crystal structures for **1** (0.0°) and **4** (49.7°). This discrepancy can probably be attributed to packing forces. The packing structures of dimers **1**–**4** in the crystals are all one-dimensional on-top π-stacks, with intermolecular distances of 3.72–3.79 Å (Figures 2b and 3c, see also Figures S24 and S27 in the Supporting Information), thus suggesting that compounds with this quasiplanar structural motif share a general tendency for the observed packing mode. DFT calculations at the B3LYP/6-31G(d) level suggested an inversion barrier for the flipping of the two phenyl rings in monomer **8a** of 9.1 kcal mol$^{-1}$ (see Figure S19 in the Supporting Information), which indicates that it should proceed easily in solution or under sublimation conditions. This flexibility should facilitate dense π-stacking in the on-top mode.

Interestingly, **2** exhibited crystalline polymorphism. Recrystallization of **2** from toluene (110–120°C) resulted in the deposition of needlelike crystals ($P\bar{1}$), containing one-dimensional on-top π-stacks of **2** along the short *a*-axis (Figure 3a,c), similar to **1**, **3**, and **4**. On the other hand, recrystallization from *o*-dichlorobenzene at higher temperature (140–160°C) or sublimation (265°C, 0.1 mmHg) provided platelike crystals ($P2_1/a$), in which two-dimensional π-stacks of **2** with a slipped arrangement were observed (Figure 3b,d). A determination of the face index confirmed that the longest axis in both types of crystals corresponds to the *a*-axis in the π-stacking direction (see Figure S29 in the Supporting Information). Since neither a phase transition between the two crystals, nor a difference in the melting point could be observed, we assume that the platelike crystals form by entropy-driven processes at higher temperature.

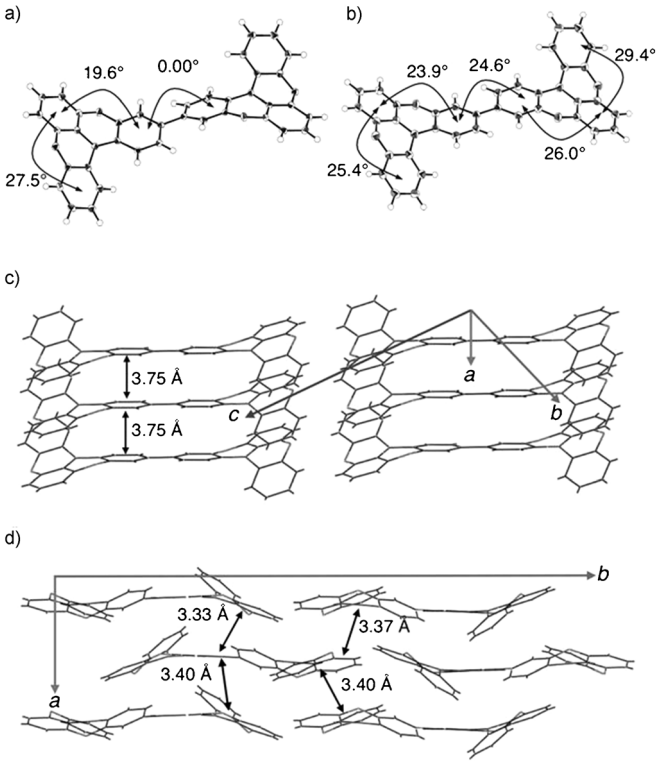


***Figure 3.*** X-ray crystal structures of **2**: ORTEP drawings (50% probability for thermal ellipsoids) and packing structures for crystals obtained from toluene (a,c) and from *o*-dichlorobenzene (b,d).

To gain insight into the relationship between packing structures and carrier-transport properties, we conducted theoretical calculations at the PW91/DZP level and evaluated the charge-transfer integrals ($J$) for crystals of **2** with different packing modes. For the one-dimensional π-stacking structure shown in Figure 3c, a large $J$ value (198 meV) was obtained for the hole-transfer integral in the direction of the on-top π-stacking (*a*-axis), whereas small values were observed in the other directions (0.72–12.8 meV). For the two-dimensional π-stacking structure shown in Figure 3d, only moderate $J$ values (4.8–27.0 meV) were obtained, with less anisotropy in all

possible directions (see Tables S2 and S3 in the Supporting Information).

To examine the relationship between packing structures and carrier-transport properties experimentally, time-resolved microwave conductivity (TRMC) measurements[11] were carried out on several dozens of crystals aligned on a quartz substrate (Figure 4a,b). TRMC measures the local mobility of charge carriers ($\phi\Sigma\mu$) under an oscillating micro-

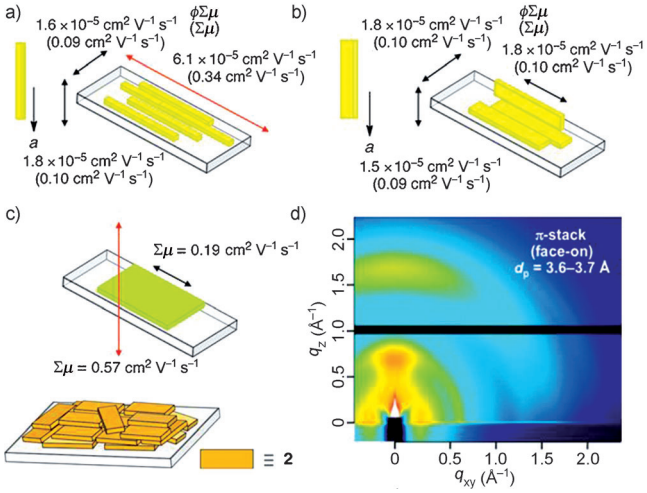


***Figure 4.*** Anisotropy of the carrier mobility measured by TRMC for a) needle-like crystals, b) platelike crystals and c) vacuum-deposited films of **2** under excitation at 355 nm. d) 2D GIXD image of a vacuum-deposited film of **2**.

wave electric field in the absence of contact between the semiconductors and the metal of electrodes, where $\phi$ is defined as the charge carrier generation efficiency. It should be noted that the local mobility ($\Sigma\mu$) obtained by TRMC is different from the bulk mobility in time-of-flight (TOF), space-charge-limited current (SCLC), and organic field-effect transistor (OFET) measurements, as the absence of the contact between the semiconductors and the electrode in TRMC measurements allows the evaluation of the intrinsic charge carrier mobility and its anisotropy.[11] Significant anisotropy of the intrinsic charge carrier mobility was observed in the crystals with one-dimensional π-stacking. It was substantially higher in the direction of the on-top π-stacking ($\phi\Sigma\mu = 6.1\times10^{-5}$ cm$^2$ V$^{-1}$ s$^{-1}$; $\Sigma\mu =$ 0.34 cm$^2$ V$^{-1}$ s$^{-1}$ [12]) compared to the other directions ($\phi\Sigma\mu =$ 1.6–1.8 $\times10^{-5}$ cm$^2$ V$^{-1}$ s$^{-1}$; $\Sigma\mu =$ 0.09–0.10 cm$^2$ V$^{-1}$ s$^{-1}$ [12]). No such anisotropy was observed in the crystals with two-dimensional π-stacks ($\phi\Sigma\mu =$ 1.5–1.8 $\times10^{-5}$ cm$^2$ V$^{-1}$ s$^{-1}$; $\Sigma\mu =$ 0.09–0.10 cm$^2$ V$^{-1}$ s$^{-1}$ [12]). These results are consistent with the hole-transfer integrals.

In many of the organic electronic devices such as OLEDs and OPVs, the charge-transporting materials are used in the form of films. Therefore, we also conducted TRMC measurements on vacuum-deposited films (100 nm thickness) of **1** (see Figure S31 in the Supporting Information) and **2** on a quartz substrate (Figure 4c). Interestingly, we also observed a significant anisotropy of the carrier mobility. The mobility in the direction perpendicular ($\Sigma\mu_{per}$) to the quartz substrate (**1**: 0.98 cm$^2$ V$^{-1}$ s$^{-1}$; **2**: 0.57 cm$^2$ V$^{-1}$ s$^{-1}$) was approximately three times higher than that in the direction parallel ($\Sigma\mu_{par}$) to the substrate (**1**: 0.38 cm$^2$ V$^{-1}$ s$^{-1}$; **2**: 0.19 cm$^2$ V$^{-1}$ s$^{-1}$). To validate that the quasiplanar structure of **1** and **2** is responsible for this anisotropy, we conducted TRMC control measurements on vacuum-deposited films of TPD, which has a corresponding nonplanar structure (see Figure S32 in the Supporting Information). However, a minimal anisotropy of the carrier mobility was observed for this TPD film ($\Sigma\mu_{per} =$ 0.53 cm$^2$ V$^{-1}$ s$^{-1}$; $\Sigma\mu_{par} = 0.37$ cm$^2$ V$^{-1}$ s$^{-1}$; $\Sigma\mu_{per}/\Sigma\mu_{par} = 1.4$); it was significantly less prominent than those in films of **1** ($\Sigma\mu_{per}/\Sigma\mu_{par} = 2.6$) and **2** ($\Sigma\mu_{per}/\Sigma\mu_{par} = 3.0$).

To confirm this anisotropy, the ordering structure of **2** in thin film was investigated by X-ray diffraction studies. Vacuum-deposited films of **2** did not exhibit any distinct diffraction peaks in measurements using a laboratory X-ray diffractometer with a sealed-tube X-ray generator (RIGAKU Ultima IV; see Figure S33 in the Supporting Information), which suggests that these films are essentially amorphous. However, in the two-dimensional grazing-incidence X-ray diffraction (2D GIXD), and using a synchrotron radiation source,[3e] we observed a diffraction halo corresponding to the π-stacking along the $q_z$-axis (out-of-plane; $q = 1.69$–$1.74$ Å$^{-1}$, Figure 4d), whereas no distinct diffraction was observed in the direction of the $q_{xy}$-axis (in-plane). The determined π-stacking distance ($d_\pi$) of 3.6–3.7 Å is in good agreement with the results obtained from the crystal structures. This finding suggests a horizontal molecular orientation (face-on), in which the π-stacking structure was retained to some extent, even in the amorphous state.[13] These results accordingly support the anisotropy of the carrier mobility observed by TRMC. In contrast, on the basis of variable angle spectroscopic ellipsometry measurements, nonplanar TPD was reported to be randomly oriented in vacuum-deposited films under similar conditions.[13b] It is therefore feasible to conclude that the anisotropy of the carrier mobility is most likely enhanced by the quasiplanar structural motif of oxygen-bridged triarylamines **1** and **2**.

In summary, we demonstrated that quasiplanar structures can be used as the key feature in the molecular design of triarylamines to obtain delocalized HOMOs and on-top π-stacks in the crystalline state, which leads to the observed high and anisotropic carrier mobilities in the π-stacking direction. We also found that these compounds retain some degree of the face-on π-stacking in amorphous films, thus facilitating out-of-plane charge transport. The properties exhibited by these quasiplanar triarylamine model compounds are expected to be extraordinarily beneficial for charge-transporting materials in OLEDs, OPVs, and perovskite-sensitized solar cells,[14] all of which require high levels of out-of-plane charge transport. Investigations concerning the applications of these types of charge-transporting materials are currently in progress in our laboratory and the results will be reported in due course.

Received: January 4, 2014
Revised: March 8, 2014
Published online: April 24, 2014

  

**Keywords:** amorphous materials · heterocycles · semiconductors · structure–function relationships · structure elucidation

[1] a) Y. Shirota, H. Kageyama, *Chem. Rev.* **2007**, *107*, 953 – 1010; b) L. Xiao, Z. Chen, B. Qu, J. Luo, S. Kong, Q. Gong, J. Kido, *Adv. Mater.* **2011**, *23*, 926 – 952.

[2] a) J. E. Anthony, *Angew. Chem.* **2008**, *120*, 460 – 492; *Angew. Chem. Int. Ed.* **2008**, *47*, 452 – 483; b) H. Klauk, *Chem. Soc. Rev.* **2010**, *39*, 2643 – 2666; c) C. Wang, H. Dong, W. Hu, Y. Liu, D. Zhu, *Chem. Rev.* **2012**, *112*, 2208 – 2267.

[3] a) B. Walker, C. Kim, T.-Q. Nguyen, *Chem. Mater.* **2011**, *23*, 470 – 482; b) A. Facchetti, *Chem. Mater.* **2011**, *23*, 733 – 758; c) A. Mishra, P. Bäuerle, *Angew. Chem.* **2012**, *124*, 2060 – 2109; *Angew. Chem. Int. Ed.* **2012**, *51*, 2020 – 2067; d) R. S. Kularatne, H. D. Magurudeniya, P. Sista, M. C. Biewer, M. C. Stefan, *J. Polym. Sci. Part A* **2013**, *51*, 743 – 768; e) I. Osaka, T. Kakara, N. Takemura, T. Koganezawa, K. Takimiya, *J. Am. Chem. Soc.* **2013**, *135*, 8834 – 8837.

[4] V. Coropceanu, J. Cornil, D. A. S. Filho, Y. Olivier, R. Silbey, J.-L. Brédas, *Chem. Rev.* **2007**, *107*, 926 – 952.

[5] D. Holmes, S. Kumaraswamy, A. J. Matzger, K. P. C. Vollhardt, *Chem. Eur. J.* **1999**, *5*, 3399 – 3412.

[6] a) J. E. Anthony, J. S. Brooks, D. L. Eaton, S. R. Parkin, *J. Am. Chem. Soc.* **2001**, *123*, 9482 – 9483; b) X. Zhang, A. P. Coté, A. J. Matzger, *J. Am. Chem. Soc.* **2005**, *127*, 10502 – 10503; c) Q. Miao, X. Chi, S. Xiao, R. Zeis, M. Lefenfeld, T. Siegrist, M. L. Steigerwald, C. Nuckolls, *J. Am. Chem. Soc.* **2006**, *128*, 1340 – 1345.

[7] a) *N*,*N*′-Diphenyl-*N*,*N*′-di(*m*-tolyl)benzidine: Z. Zhang, Z. E. Burkholder, J. Zubieta, *Acta Crystallogr. Sect. C* **2004**, *60*, o452 – o454; b) 4,4-bis[*N*-(1-naphthyl)-*N*-phenylamino]biphenyl: L.-Q. Huang, Q.-Y. Cao, C. Yi, C.-J. Yang, X.-C. Gao, *Acta Crystallogr. Sect. E* **2006**, *62*, o2075 – o2076.

[8] T. Yamada, T. Sato, K. Tanaka, H. Kaji, *Org. Electron.* **2010**, *11*, 255 – 265.

[9] M. Kuratsu, M. Kozaki, K. Okada, *Chem. Lett.* **2004**, *33*, 1174 – 1175.

[10] J. Pommerehne, H. Vestweber, W. Guss, R. F. Mahrt, H. Bässler, M. Porsch, J. Daub, *Adv. Mater.* **1995**, *7*, 551 – 554.

[11] a) A. Saeki, Y. Koizumi, T. Aida, S. Seki, *Acc. Chem. Res.* **2012**, *45*, 1193 – 1202, and references therein; b) A. Saeki, S. Seki, T. Takenobu, Y. Iwasa, S. Tagawa, *Adv. Mater.* **2008**, *20*, 920 – 923; c) Y. Yasutani, A. Saeki, T. Fukumatsu, Y. Koizumi, S. Seki, *Chem. Lett.* **2013**, *42*, 19 – 21.

[12] The charge carrier generation efficiency ($\phi = 1.76 \times 10^{-4}$ for **2**) was measured for the vacuum-deposited film and was subsequently used to estimate the local mobility $\Sigma\mu$ in the crystals.

[13] a) D. Yokoyama, *J. Mater. Chem.* **2011**, *21*, 19187 – 19202, and references therein; b) D. Yokoyama, A. Sakaguchi, M. Suzuki, C. Adachi, *Appl. Phys. Lett.* **2008**, *93*, 173302.

[14] a) A. Kojima, K. Teshima, Y. Shirai, T. Miyasaka, *J. Am. Chem. Soc.* **2009**, *131*, 6050 – 6051; b) M. M. Lee, J. Teuscher, T. Miyasaka, T. N. Murakami, H. J. Snaith, *Science* **2012**, *338*, 643 – 647; c) J. H. Heo, S. H. Im, J. H. Noh, T. N. Mandal, C.-S. Lim, J. A. Chang, Y. H. Lee, H. Kim, A. Sarkar, M. K. Nazeeruddin, M. Grätzel, S. I. Seok, *Nat. Photonics* **2013**, *7*, 486 – 491.

  